Paper-302-21

19th International Conference on Renewable Energies and Power Quality (ICREPQ'21)
Almeria (Spain), 28th to 30th July 2021
Renewable Energy and Power Quality Journal (RE&PQJ)
ISSN 2172-038 X, Volume No.19, September 2021

Performance evaluation of high-lift hydrofoils with a flap used in the design of horizontal-axis hydrokinetic turbines

Rubio-Clemente A.[1,2], Aguilar J.[2], Chica E.[2]

[1] Facultad de Ingenierías, Universidad de Medellín, Carrera 87, No. 30-65, Medellín, Colombia.
[2] Grupo de Investigación Energía Alternativa, Facultad de Ingeniería, Universidad de Antioquia UdeA, Calle 70, No. 52-21, Medellín, Colombia.
Phone/Fax number: +57(4)3405555, e-mail: arubio@udem.edu.co

Research problem

The hydrodynamic performance and the flow field of two horizontal-axis hydrokinetic turbines with and without a high-lift hydrofoil including a flap were investigated using computational fluid dynamics (CFD) simulation. For improving the accuracy of the numerical simulation, the user-defined function (UDF) of 6-degrees of freedom (6-DoF) was used in the Ansys Fluent software. Unsteady Reynolds-Averaged Navier–Stokes (URANS) equations coupled to the SST $k-\omega$ turbulence model were employed during the simulation. A three-dimensional model of the turbines with three blades was conducted for obtaining the performance curve of the power coefficient (C_P) *versus* the tip speed ratio (TSR). The maximum power coefficients ($C_{P_{Max}}$) of the hydrokinetic turbines with and without a high-lift hydrofoil arrangement were 0.5050 and 0.419, respectively. Experimental data from the literature were used for the validation of the numerical results, specifically for the case when a rotor with traditional blades is utilized. In general, the simulation results were in good agreement with the experimental data.

Keywords: Hydrofoil-flap arrangement, 6-DoF, hydrokinetic turbine, high-lift hydrofoil, Richardson extrapolation.

Material and methods

r/R	β (°)	C/R
0.1	50.83	0.05949
0.2	35.93	0.05063
0.3	27.35	0.04050
0.4	22.18	0.03291
0.5	18.82	0.02785
0.6	16.48	0.02405
0.7	14.77	0.02152
0.8	13.46	0.01899
0.9	12.43	0.01772
1.00	11.61	0.01646

The design of the rotors was carried out using the blade element momentum theory (BEM)

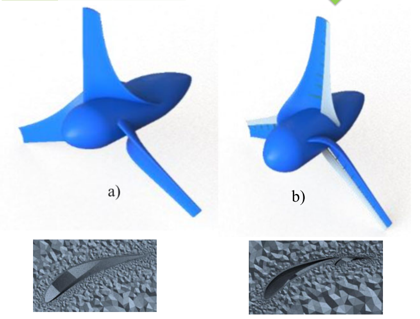

Figure. 1. Solid view of the rotors. a) Traditional rotor and b) high-lift rotor

Objective

The goal of this work is to perform a numerical investigation on the effect of a high-lift hydrofoil with a flap on a horizontal-axis hydrokinetic turbine using the 3D CFD technique, including the UDF of 6-DoF. For this purpose, the numerical results obtained are compared and discussed based on the experimental data available in the literature on the performance of a horizontal-axis hydrokinetic turbine whose blade has been designed with a hydrofoil traditional configuration (Figure 1).

$$\omega = \int \frac{M_F - M_A}{J} dt$$

$$P = M_A \omega$$

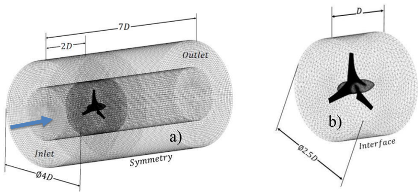

Figure. 2. a) Computational domain and b) inner cylindrical rotatory zone

Table 1. Parameters involved in the CFD analysis.

Parameter (units)	Description
Blade profile	Eppler 420
Diameter rotor (D)	1.58 m
Radius (R) rotor	0.79 m
Fluid	Water at 25 °C
Turbulence model	$k-\omega$ SST
Inlet	Velocity inlet (1.5 m/s)
Outlet	Pressure outlet
Wall of the external cylinder	Symmetric boundary
Hydrofoil	No-slip wall

Richardson extrapolation method

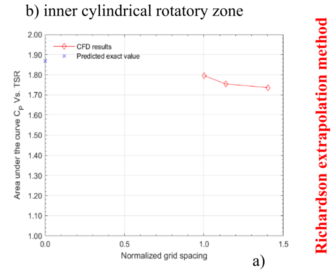

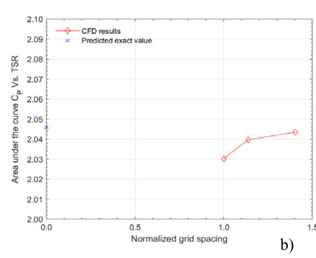

Figure 3. Mesh independence test results. a) Traditional rotor and b) high-lift rotor

Results and discussion

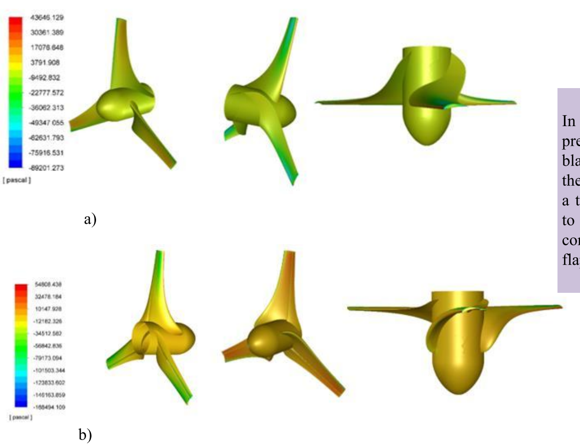

Figure 4. Pressure contours of (a) the traditional hydrofoil and (b) the hydrofoil-flap arrangements

In the pressure distributions, the pressure was negative on the blade suction side and positive on the pressure side. The blade with a traditional hydrofoil was found to provide higher pressures in comparison with the hydrofoil-flap arrangements.

Fig. 5 shows the distribution of C_P with different values of TSR using the CFD approach and the experimental results reported in the literature. The numerical results for the traditional rotor were in good agreement with a previous study of this specific turbine model in terms of similar C_P values, except that the C_P peak was achieved at a different TSR value. The differences are due to the fact that the hydrofoil used in the study of Tian and co-workers was the FF-77-W airfoil type.

$$C_P = \frac{P}{\frac{1}{2}\rho V^3 \pi R^2}$$

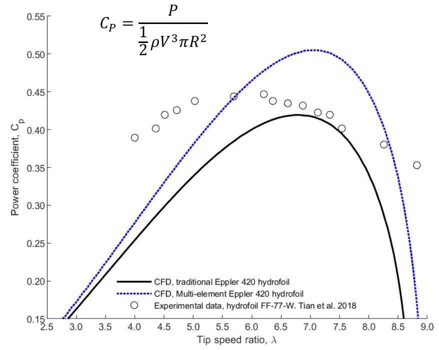

$$TSR = \frac{\omega R}{V}$$

Figure. 5. Variation of the power coefficient (C_P) *vs.* the tip speed ratio (TSR)

The maximum C_P values obtained were 0.505 and 0.419 for the high-lift hydrofoil and the traditional configurations, respectively.

Conclusion

Using URANS solver and 6-DOF function, 3D CFD studies were conducted to predict the performance of two rotors, defined by the C_P achieved at different TSR values. The results demonstrated that the rotor with a high-lift hydrofoil enhanced the C_P compared to the rotor with a single-element hydrofoil arrangement. From the 3D CFD analyses for the high-lift hydrofoil, the maximum efficiency found was 0.5050, while a maximum efficiency of 0.419 was obtained with the traditional hydrofoil configuration. The validation showed that the CFD results concerning the traditional hydrofoil configuration were in good agreement with the empirical data examined. In this study, grid convergence index (GCI) was a good option for estimating the appropriate sizes of the time-step and the mesh.

Nomenclature

D: diameter of the rotor
R: radius of the rotor
r: location of each cross-section from the hub
β: blade twists angle
C: chord length of the hydrofoil
P: mechanical power output
ρ: fluid density
V: incoming velocity
ω: angular velocity
M_F: total hydrodynamic moment acting on the turbine blade
M_A: applied moment on the rotational axis for determining the power of the turbine

References

[1] Maldar, N. R., Ng, C. Y., and Oguz, E. A review of the optimization studies for Savonius turbine considering hydrokinetic applications. Energy Conversion and Management (2020). Vol. 226, 113495.
[2] Lust, E. E., Bailin, B. H., and Flack, K. A. Performance characteristics of a cross-flow hydrokinetic turbine in current only and current and wave conditions. Ocean Engineering (2021). Vol. 219, 108362.
[3] John, B., and Varghese, J. Sizing and techno-economic analysis of hydrokinetic turbine based standalone hybrid energy systems. Energy (2021). Vol. 221, 119717.
[4] Yuce, M. I., and Muratoglu, A. Hydrokinetic energy conversion systems: A technology status review. Renewable and Sustainable Energy Reviews (2015). Vol. 43, pp. 72-82.
[5] Kirke, B. Hydrokinetic turbines for moderate sized rivers. Energy for Sustainable Development (2020). Vol. 58, pp. 182-195.
[6] Narsipur A., Pomeroy B., and Selig M. CFD Analysis of multielement airfoil for wind turbines. 30th AIAA Applied Aerodynamics Conference (2012). pp. 2781.
[7] Yavuz, T., Kilkis, B., Koc, E., and Erol, O. Flow and performance characteristics of a double-blade hydrofoil. In Advanced Materials Research (2012). Vol. 433, pp. 7218-7222.
[8] Yavuz, T., and Koç, E. Performance analysis of double blade airfoil for hydrokinetic turbine applications. Energy conversion and management (2012). Vol. 63, pp. 95-100.
[9] Yavuz, T., Koç, E., Kılkış, B., Erol, Ö., Balas, C., and Aydemir, T. Performance analysis of the airfoil-slat arrangements for hydro and wind turbine applications. Renewable energy (2015). Vol. 74, pp. 414-421.
[10] Hashemi, S. M., Moghimi, M., and Derakhshan, S. Experimental and numerical study of a flapping-blade vertical-axis hydrokinetic turbine under free surface deformation and blockage effects. International Journal of Environmental Science and Technology (2020). Vol. 17(8), pp. 3633-3650.
[11] Ragheb, A., and Selig, M. Multi-element airfoil configurations for wind turbines. In 29th AIAA Applied Aerodynamics Conference (2011). pp. 3971.
[12] Aguilar, J., Rubio-Clemente, A., Velasquez, L., and Chica, E. Design and Optimization of a Multi-Element Hydrofoil for a Horizontal-Axis Hydrokinetic Turbine. Energies (2019). Vol. 12(24), pp. 4679.
[13] Jeong, S., Murayama, M., and Yamamoto, K. Efficient optimization design method using kriging model. Journal of aircraft (2005). Vol. 42(2), pp. 413-420.
[14] Manwell, J. F., McGowan, J.G., and Rogers, A.L. Aerodynamics of Wind Turbines. In: J. F Manwell, JG McGowan and AL Rogers (eds) Wind energy explained: theory, design and application. 2th ed. UK: John Wiley & Sons 2009, cap. 3, pp. 91-155.
[15] Menter, F.R. Two-equation eddy-viscosity turbulence models for engineering applications. AIAA journal (1994). Vol. 32(8), pp. 1598-1605.
[16] Prakoso, A. P., Adanta, D., and Irwansyah, R. Approach for a breastshot waterwheel numerical simulation methodology using six degrees of freedom. Energy Reports (2020). Vol. 6, pp. 611-616.
[17] Prakoso, A. P., Siswantara, A. I., and Adanta, D. Comparison between 6-DOF UDF and moving mesh approaches in CFD methods for predicting cross-flow pico-hydro turbine performance. CFD Letters (2019). Vol. 11(6), 86-96.
[18] Roache, P. J. Perspective: a method for uniform reporting of grid refinement studies. Journal of Fluids Engineering (1994). Vol. 116, pp. 405-413.
[19] Tian, W., Mao, Z., and Ding, H. Design, test and numerical simulation of a low-speed horizontal axis hydrokinetic turbine. International Journal of Naval Architecture and Ocean Engineering (2018). Vol. 10(6), pp. 782-793